

紫外線と水による福島県川俣町水晶山産鉄カンラン石の変質 Change in fayalites with ultraviolet rays and water

小森 信男^{1*}
KOMORI, Nobuo^{1*}

¹ 大田区立蒲田中学校

¹ Kamata junior high school

筆者は、2年前のこの大会で、八丈島産鉄かんらん石の紫外線と水による鉄カンラン石の変質について報告した。その後同様の実験を、福島県川俣町水晶山産鉄カンラン石で行ってみた。

福島県川俣町産鉄カンラン石は、全体として暗緑色を呈している。鉄カンラン石試料は、福島県川俣町水晶山産のものであり、地質関連の業者2社(A社B社とする)からそれぞれ50g程購入したものをハンマーで砕き、2g前後の塊状の試料にしたものである。試料はその後、表面についている微粉末を取り除くために、水道水に浸し3分間の超音波洗浄を4回行った後、精製水に浸し3分間の超音波洗浄を1回行った。A社のものは、野外における風化の程度がそれほど進んでおらず新鮮な面が多い。この試料を試料Aとした。B社のものは風化がある程度進み、表面が赤褐色に変色した部分が多い。この試料を試料Bとして、どちらも次の実験を行った。

精製水を満たした石英試験管に2g程の塊状の鉄カンラン石を入れた。そして254nmをピークとする紫外線を照射した。対照実験として、同じ条件で紫外線を照射しない実験も行った。紫外線は3ヶ月照射した。なお、照射開始時の照度は40W/m²程である。

その結果、試料Bの紫外線を照射したものには、褐色の0.1mm以下の微粒子が多数生じた。この微粒子は、XRDによる分析から、マグヘマイト、水酸化鉄、二酸化マンガンの3種が含まれている可能性があることがわかった。試料Bの紫外線を照射しないものは、ほとんど変化はなかった。試料Aでは、紫外線を照射した方もしない方も、ほとんど変化はなかった。

野外における風化の進んだ試料Bの場合は、水中に溶け出る鉄イオンの量が多く、紫外線と水のはたらきで、鉄イオンの酸化が促進され、酸化鉄の粉末が多く生じたと推定している。一方、試料Aの場合は、水中に溶け出る鉄イオンの量が少なく、紫外線を照射しても酸化鉄はほとんど生じないと推定した。

キーワード: 紫外線, 水, 鉄カンラン石, 水酸化鉄, マグヘマイト, 変質
Keywords: ultraviolet rays, water, fayalite, iron oxide, maghemite, change

forsterite における炭素溶解メカニズムの解明 Carbon dissolution mechanism in forsterite

三谷 彩木^{1*}; 興野 純¹
MITANI, Saki^{1*}; KYONO, Atsushi¹

¹ 筑波大学大学院生命環境科学研究科地球進化科学専攻

¹ Graduate School of Life and Environmental Sciences, University of Tsukuba

はじめに

珪酸塩鉱物は地殻・マントル中を構成する主要な鉱物であり、地球内部において重要な役割を担っている。また、炭素も地球内部に多量に存在し、珪酸塩鉱物中にわずかに固溶することが知られている。Shcheka et al. (2006) は、高温高压実験によってマントル鉱物への炭素溶解度を調べ、olivine では圧力が上昇するに伴って炭素溶解度は増加し、11 GPa で最大 12 ppm 溶解することを示した。このとき炭素は C^{4+} とし Si^{4+} と置換し、olivine の SiO_4 四面体内に CO_4 四面体として占有される可能性を示唆した。また、Sen et al. (2013) は非晶質のオキシ炭化ケイ素 ($SiOC$) の PDCs (Polymer-Derived Ceramics) を用いた実験によって、地球環境下では炭素と酸素の置換が低温高压領域の珪酸塩鉱物中で発生することを指摘し、熱力学的には炭素は Si^{4+} と置換するより酸素と置換しやすいことを明らかにした。このように、珪酸塩鉱物に炭素が溶解するとき、炭素は Si^{4+} の原子位置に取り込まれ CO_4 四面体となるのか、酸素の原子配置に占有され SiC_4 四面体となるのか、一部の酸素と置換し $Si(O,C)_4$ 四面体となるのか、その特性はまだ完全には明らかになっていない。

そこで、本研究では上部マントルの主要構成鉱物である forsterite における炭素置換メカニズムを解明することを目的とする。

実験方法

炭素溶解実験に使用した鉱物試料は、天然の forsterite (San Carlos, California, USA) である。Forsterite と炭素の反応剤 (graphite または活性炭) をそれぞれ混合し粉末にしたものを石英ガラスチューブに入れ真空封入し、1000 °C、2 日間加熱した。加熱後、粉末 XRD 測定によって生成物の格子定数の変化を調べた。赤外線吸収スペクトルでは SiO_4 四面体における分子の伸縮運動の変化から炭素が SiO_4 四面体に取り込まれた否かを分析した。EPMA 測定では生成物の炭素の定量分析を行った。さらに、第一原理計算によって生成物の構造の推定を行った。

結果・考察

粉末 XRD 測定より、炭素の増加に伴って b 値、 c 値の長さが収縮し、単位格子の体積が減少するという傾向があった。赤外線吸収スペクトル分析より、 $C-O$ 結合の伸縮振動が現れるスペクトルの領域にわずかなショルダーが見られた。EPMA 測定からは炭素が有意に認められ、反応前後で Si と C のイオン数に負の相関が認められた。第一原理計算より、炭素は SiO_4 四面体中の Si と置換して $C-O$ 結合を形成したときがエネルギー的に安定した。 $Si-O$ 結合の距離と置換後の $C-O$ 結合の距離を比較すると、結合距離は明らかに短くなった。本研究の結果から、forsterite には炭素を溶解することが可能であるということが示唆される。さらに、このとき炭素が SiO_4 四面体内の Si^{4+} と置換していることが考えられる。

しかしながら、個々の Forsterite 中で置換する炭素の量はわずかであるため、今後慎重な検証実験を繰り返し、結論を導くことが必要である。

キーワード: 珪酸塩鉱物, 炭素溶解, フォルステライト

Keywords: silicate mineral, carbon dissolution, forsterite

高压下における KAlSi_3O_8 メルトの粘度 Viscosity of KAlSi_3O_8 melt under high pressure

鈴木 昭夫^{1*}
SUZUKI, Akio^{1*}

¹ 東北大学大学院理学研究科地学専攻
¹Tohoku University

マグマは一般に地球内部の高温高压力下で発生して地表へと噴出する。このため、高温高压力下でのマグマの物性を知ることは重要である。これまで行われてきた研究により、マグマ（ケイ酸塩メルト）には圧力の増加と共に粘度が減少する物と増加する物があることが知られている。この様な違いはメルトの構造の違いおよび圧力の増加に伴う構造変化の違いで説明されているが、不明な点も多い。常圧下でネットワーク構造が発達しているメルトは圧力の増加に伴って粘度が減少するが、例えば $\text{NaAlSi}_2\text{O}_6$ 組成のメルトでは 2GPa 以上で粘度がほぼ一定になる (Suzuki et al., 2011)。高压力下でのマグマの粘度を理解するには、さらに多様な組成かつ広範な温度圧力下で調べる必要がある。

KAlSi_3O_8 は長石の端成分で、White and Montana (1990) によって 2.5 GPa まで粘度測定が行われた。彼らの結果によると、1500 °C では 2 GPa で粘度が極小になるのに対し、1600 °C では 2.5 GPa まで単調に減少することが報告されている。すなわち、粘度の温度依存性は 2.0 GPa 以下と 2.5 GPa で大きく異なることを意味しているが、筆者による $\text{NaAlSi}_2\text{O}_6$ メルトの粘度測定からは、およそ 3 GPa まで粘度の温度依存性に変化はないことが示されている。そこで本研究では、 KAlSi_3O_8 組成のメルトの粘度を高温高压力下で測定し、粘度の温度圧力依存性を調べた。

実験は茨城県つくば市にある高エネルギー加速器研究機構 (KEK) の放射光実験施設である PF-AR リングの NE7A ステーションでおこなった。NE7A にはマルチアンビル型高压発生装置 MAX-III が備え付けてある。粘度測定は X 線イメージング落球法でおこなった。高温高压下において、高压セルに放射光 X 線を照射し、試料中を落下する白金球の X 線動画イメージから落下速度を測定して粘度を算出した。試料には天然のサニディン (KAlSi_3O_8) を使用した。実験は約 6GPa までの圧力下で行った。

実験の結果、約 6GPa まで粘度が単調に減少することがわかった。また、粘度の温度依存性は、約 6GPa までほぼ一定であった。White and Montana (1990) で報告された粘度極小は認められなかった。本研究との違いをもたらした原因は不明だが、詳細は当日述べる。

キーワード: マグマ, 粘度, 高压, マントル, 放射光

Keywords: magma, viscosity, high pressure, mantle, synchrotron radiation

球共振法により求めた石英単結晶の弾性定数および温度依存性
Elastic constants of single-crystal quartz and their temperature dependence studied via
sphere-resonance method

瀬間 文絵^{1*}; 渡辺 了¹

SEMA, Fumie^{1*}; WATANABE, Tohru¹

¹ 富山大学大学院理工学教育部

¹Graduate School of Science and Engineering, University of Toyama

Single-crystal elastic constants of rock-forming minerals and their temperature dependence are critical for interpreting observed seismic velocities. A good interpretation requires a thorough understanding of elastic properties of major constituent minerals. Compared with mantle minerals such as olivine, to which a lot of work have been done, elastic properties of crustal minerals have been poorly constrained. Quartz is one of the most abundant minerals in the crust. We have studied elastic constants of single-crystal quartz and their temperature dependence by the sphere-resonance method.

A sphere sample (D=5.826(1) mm) was made from a synthetic quartz single-crystal by the two-pipe method. Resonant frequencies were measured with ultrasonic transducers (Panametrics, V156RM), a lock-in-amplifier (SRS, SR844) and a function generator (Tektronix, AFG320). Measurements were made at frequencies from 400 kHz to 1.2 MHz with different specimen-holding forces. Extrapolating to the specimen-holding force of zero, we obtained frequencies of "free" oscillation. The sample and transducers were placed in a temperature-controlled container. The temperature was changed from 0 to 40°C. Elastic constants were determined by comparing measured and calculated resonant frequencies. The xyz algorithm (Visscher et al., 1991) was employed to calculate resonant frequencies of the sphere sample. Preliminary analysis has shown that C₁₁, C₃₃, C₄₄, C₁₂, C₁₃ and C₁₄ at room temperature (19.4°C) are 87.224, 105.47, 58.328, 6.885, 11.914, 18.116 (GPa), respectively. The temperature dependence of elastic constants will also be presented in this poster.

キーワード: 弾性定数, 共振法, 温度依存性, 石英

Keywords: elastic constants, resonance method, temperature dependence, quartz

ブルーサイトとポートランダイト中のプロトンダイナミクスの速度論的研究 A kinetical study of proton dynamics of brucite and portlandite

増田 愛美¹; 永井 隆哉^{2*}; 川野 潤²
MASUDA, Manami¹; NAGAI, Takaya^{2*}; KAWANO, Jun²

¹ 北海道大学大学院理学院, ² 北海道大学大学院理学研究院

¹School of Science, Hokkaido University, ²Faculty of Science, Hokkaido University Graduate

Brucite is $Mg(OH)_2$ compound and the crystal structure of brucite is recognized as a prototype of hydrous layered minerals with complicated structures. Various physical and chemical properties of some minerals with the brucite structure such as brucite itself and portlandite, $Ca(OH)_2$ have been investigated. It is especially interesting to understand proton dynamics in hydrous minerals, because the proton diffusion should be closely related to mechanism and kinetics of plastic deformation, hydration, dehydration and so on. Nevertheless, proton diffusion studies on brucite structured minerals have been surprisingly scarce. Recently Noguchi and Shinoda (2010) conducted H-D exchange diffusion experiments on portlandite and Guo et al. (2013) performed proton diffusion experiments on brucite at high pressure. However, it is difficult to understand mechanism of proton diffusion of brucite structured minerals systematically, because their experimental conditions such as pressure and temperature are different. In this study, we performed deuterated experiments for brucite, hydrated experiments for deuterated brucite and deuterated experiments for portlandite at several temperatures and at an atmospheric pressure.

All sample powders were prepared by hydrothermal synthesis and checked the qualities by X-ray diffraction, infrared absorption spectroscopy and SEM. The H-D exchange experiments at several temperatures were performed with a vertical tube furnace in which bubbling dried N_2 gas through D_2O (or H_2O) was introduced. A crucible filled with the sample powder was hung in the middle of the tube furnace. A small amount of the sample powder was picked out at appropriate time intervals and IR measurements for it were performed to know time variation of the molar ratio of D to H.

The diffusion rate depends on temperature and is faster at higher temperature. The diffusion rate also depends on the molar ratio of D to H. Rate control process of proton diffusion in brucite structured minerals will be discussed from diffusion coefficients, activation energies and frequency factors determined.

キーワード: 水素拡散, 水素-重水素交換反応, ブルーサイト, ポートランダイト, 速度論的解析

Keywords: Proton dynamics, H-D exchange, brucite, portlandite, kinetics

コンドライト隕石へのラマン分光炭質物温度計の適用 Application of the Raman carbonaceous material thermometer to chondrites

本馬 佳賢^{1*}; 瀧 佑衣¹; 鍵 裕之¹; 三河内 岳¹; 藪田 ひかる²
HOMMA, Yoshitaka^{1*}; KOUKETSU, Yui¹; KAGI, Hiroyuki¹; MIKOUCHI, Takashi¹; YABUTA, Hikaru²

¹ 東京大学大学院理学系研究科, ² 大阪大学大学院理学研究科

¹Graduate School of Science, The University of Tokyo, ²Graduate School of Science, Osaka University

はじめに

炭質物の構造は、過去に受けた最高変成温度を反映するとされており、隕石の熱史解明の手掛かりとしての利用が注目されている。炭質物は地球上の堆積岩や変成岩及び始原的な隕石中に普遍的に存在するため、炭質物を温度計として利用する数多くの研究が報告されている。炭質物の構造は様々な分析法で調べられているが、当研究では非破壊的にその場計測が出来るラマン分光法に着目した。炭質物のラマンスペクトルは 1580 cm^{-1} (G-band) と 1355 cm^{-1} (D1-band) 付近に特徴的なピークを持ち、それぞれのピークの面積比や強度比、及び半値幅などは、母岩の受けた最高変成温度 (PMT: peak metamorphic temperature) と相関があることが知られている。地球上の岩石中に含まれる炭質物については、最大5本のピークを用いた詳細な解析が行われており、 $150\sim 650\text{ }^{\circ}\text{C}$ の広い範囲で温度履歴の解析が可能となっている (Kouketsu et al., 2014)。一方で、隕石に含まれる炭質物については、2本のピークによる解析しかなされていない。当研究では、地球上の岩石に含まれる炭質物に適用されている解析手法を参考にして、隕石中の炭質物ラマンスペクトルの詳細な解析を行い、隕石に適用できるラマン分光炭質物温度計の改良を試みた。

Samples and Methods

当研究では炭素質コンドライト隕石、普通コンドライト隕石、Rコンドライト隕石の20試料に含まれる炭質物についてラマンスペクトルの測定をおこなった。隕石試料のうち、14試料は岩片を、5試料は薄片を、また1試料については化学処理によって抽出された不溶性有機物を分析した。試料表面でのレーザー強度は $1\sim 2.5\text{ mW}$ に設定し、 $10\sim 30$ 秒積算した。一部の試料を除き最低30点以上測定した。得られたスペクトルはベースラインを線形として差し引いた後に4本の偽フォークト関数を用いて回帰分析を行った。ピーク分離によって得られた各ピークパラメーター (面積、強度、中心波数、半値幅) の平均をその試料のデータとした。

結果と考察

各試料について4本のピーク ($G_L, D1, D3, D4$ -band) による回帰分析を行った結果、炭質物中の結晶構造の乱れを反映しているとされる D1-band の半値幅 (Γ_{D1}) と PMT の間に相関が見られた。Huss et al. (2006) などによって変成温度の推察がなされている約 $120\text{ }^{\circ}\text{C}$ から $550\text{ }^{\circ}\text{C}$ の7つの試料を用いて検量線を作成したところ、両者の間で線形の相関式が得られた。

一方、温度未知の13試料の隕石について上記の温度計を適用してみると、 Γ_{D1} 値はある程度の高温に達すると飽和し、それ以上変化しない事が示された。この現象は Kouketsu et al. (2014) でも確認されている。今回は Allende の D1-band の半値幅 ($\Gamma_{D1} = 65\text{ cm}^{-1}$; $\text{PMT} = 550\text{ }^{\circ}\text{C}$) を検出下限と見なし、温度計の上限とした。

結論

隕石中の炭質物のラマンスペクトルを4本のピークで分離した結果、D1-band の半値幅と最高変成温度との間に線形の相関が得られた。両者の関係式を導出し、隕石に適用可能な新しいラマン分光炭質物温度計を作成した。適用可能な温度範囲は約 $200\sim 550\text{ }^{\circ}\text{C}$ である。

ピーク解析の最適条件についてはさらなる検討の余地があるが、今後さらに分析試料を増やすことで、 $200\text{ }^{\circ}\text{C}$ 以下の低変成領域に拡張できる可能性もある。

キーワード: コンドライト隕石, 炭質物, ラマン分光分析, 熱史

Keywords: chondrites, carbonaceous material, Raman spectroscopy, thermal history

分子軌道法を用いた Si-O-Si 架橋の性質の研究 Nature of Si-O bonding via molecular orbital calculation

則竹 史哉^{1*}; 河村 雄行¹
NORITAKE, Fumiya^{1*}; KAWAMURA, Katsuyuki¹

¹ 岡山大学

¹ Okayama University

Understanding the nature of Si-O bonding and Si-O-Si bridging is important for mineralogy, material science and metallurgy. It is well known that the variation of Si-O-Si angle in silicates is caused by difference of composition, temperature and pressure. The change of angle of Si-O-Si bridging affects the strength of Si-O bonding. For instance, the increase of Si-O-Si angle decreases the Si-O bond length in coesite crystal (Gibbs et al. 1977). The decrease of Si-O-Si angle of liquid silicates as a result of compression is reported by various researchers (e.g. Navrotsky et al., 1985 Ohtani et al., 1985, Sakamaki et al., 2012). The decrease of Si-O-Si angle is thought to be the trigger of decrease of viscosity of liquid silicates. (Navrotsky et al., 1985, Noritake et al., 2012). Quantum chemical properties of Si-O-Si bridging is investigated to understand the relationship between Si-O-Si angle, Si-O bond length and its strength (e.g., Newton and Gibbs 1980, Tsuneyuki 1996, Kubicki and Sykes 1993). Newton and Gibbs (1980) reports the pyrosilic acid molecule has energy minimum at Si-O-Si angle of 145° using STO-3G basis set (Hehre et al 1969) by Hartree-Fock method. Tsuneyuki (1996) reports that the bending of Si-O-Si is not reproduced using double-zeta function basis set nevertheless the increase of the number of basis function generally increase the reproducibility. However, the nature of Si-O-Si bridgings seems not to be reproduced by increase of basis function using Hartree-Fock method. In this paper, we show the molecular orbital calculation about pyrosilic acid molecule using post-Hartree-Fock method and more precise basis set to understand the nature of Si-O-Si bridging.

Molecular orbital calculations were performed using the GAUSSIAN 09 code. We firstly calculate the optimized structure of disiloxane (Almenningen et al., 1963) by Hartree-Fock (HF), second-order Moller-Plesset perturbation theory (MP2), and two density functional theory (Becke's density functional (Becke, 1988) with three correlation functionals by Lee, Yang and Parr (B3LYP) (Lee et al., 1988), and generalized gradient approximation by Perdew, Burke and Ernzerhof (PBE) (Perdew et al., 1996)) with 6-311G(d,p) split valence double zeta basis set (Raghavachari et al., 1980). The bending of Si-O-Si bridging is not reproduced by HF method as shown in Tsuneyuki (1996). The bending of Si-O-Si bridging is reproduced by use of MP2 and density functional theory with PBE. The optimized angle of Si-O-Si in disiloxane molecule by MP2 is closer to experimental value than that by PBE. Then we apply the MP2 method with 6-311G(d,p) basis set to the calculation of pyrosilic acid, H₆Si₂O₇. NBO analysis (Foster and Weinhold, 1980, Reed et al., 1985; 1988) is used to analyze the electronic state of bonding.

We found the equilibrium geometries for bended two pyrosilic acid molecules (C_{2v} and 60° torsion) using Moller-Plesset perturbation theory and with 6-311G(d,p) split valence double zeta basis set. We calculated the energy surface with varying Si-O_{br} length and Si-O-Si angle and found the relationship between Si-O_{br} length and bridging angle. From the energy surface, the stable Si-O bond length decrease with spreading Si-O-Si angle. The bending of Si-O-Si angle in equilibrium geometries can be explained by explained by the balance of Coulombic repulsion between tetrahedra and lone pair electrons of bridging oxygen atom without concerning the contribution of d-p π-bonding. The Si-O bonding strengthen with increasing Si-O-Si angle because of stabilization in energy of Si-O bonding orbital with decreasing the hybridization index λ in sp^λ orbital of bridging oxygen and increase of coulombic interaction between Si and bridging oxygen atom.

キーワード: 分子軌道法, Si-O-Si 架橋

Keywords: Molecular orbital calculation, Si-O-Si bridging

マグネサイトの構造欠陥による青色カソードルミネッセンス Blue cathodoluminescence derived from defect centers in magnesite

草野 展弘^{1*}; 西戸 裕嗣¹; 蜷川 清隆¹

KUSANO, Nobuhiro^{1*}; NISHIDO, Hirotsugu¹; NINAGAWA, Kiyotaka¹

¹ 岡山理科大学

¹ Okayama University of Science

Cathodoluminescence (CL) has been widely applied in mineralogical and petrological investigations, especially for carbonates. Although most calcite-type carbonates exhibit red to orange CL activated by divalent Mn ions, blue CL is uncommon in carbonates, but not with bright emission (e.g., Machel et al., 1991). Magnesite occasionally shows red CL emission assigned to an impurity center of divalent Mn ion substituted for an Mg ion as an activator (Medlin 1963, Sommer 1972), but not usually accompanied by blue emission. We have confirmed a significant blue emission in the CL of magnesite from Tennohama, Wakayama, Japan.

Blue luminescent magnesite (BM) occurs as a rhombohedral crystal in hydrothermal veinlets associated with dolomite and quartz. Its single crystal in size of 2-3 mm has been employed for CL measurements, as well as a single crystal of common magnesite (RM) with red CL emission from Brumado, Brazil. Color CL images were obtained using a cold-cathode type Luminescence microscope with a cooled-CCD camera. CL spectroscopy was made by a SEM-CL system, which is comprised of SEM (JEOL: JSM-5410LV) combined with a grating monochromator (OXFORD: Mono CL2). The CL emitted from the samples was dispersed by a grating monochromator (1200 grooves/mm), and recorded by a photon counting method using a photomultiplier tube. All CL spectra were corrected for total instrumental response, which was determined by use of a calibrated standard lamp.

BM spectrum shows an enhanced broad-band emission with triplet peaks from 300-400 nm in a blue region and a broad-band emission at ~670 nm in a red region, whereas RM has an intense broad band emission at ~670nm previously reported in magnesite samples (e.g., Sommer, 1972) and no emission in a blue region. Blue CL emissions of BM is possibly to be the "background blue" found in the calcite contained almost no activator (Richter and Zinkernagel, 1981), which might be related to an intrinsic defect center. In the case of BM, its emission band in a blue region has triplet peaks with high intensity, but a single broad band with low intensity for calcite.

Therefore, a Gaussian fitting of BM spectrum in an energy unit successfully deconvolutes three emission components at around 2.52 eV (492 nm), 3.28 eV (378 nm) and 3.88 eV (320nm) in a blue region. Kusano et al. (2014) reported a blue CL emission in the calcite with emission components at 2.67eV (464nm) and 3.30eV (376nm), which is the material decomposed from dolomite in the process of skarn mineralization at high temperature. It suggests that the CL derived from defect centers in BM might be attributable to its thermal history during crystal growth.

キーワード: マグネサイト, カソードルミネッセンス, 青色発光, 構造欠陥

Keywords: magnesite, cathodoluminescence, blue emission, defect center

隕石中に見出されるエンスタタイトのカソードルミネッセンス特性 Cathodoluminescence characterization of enstatite in meteorites.

大郷 周平^{1*}; 西戸 裕嗣¹; 蜷川 清隆¹
OHGO, Syuhei^{1*}; NISHIDO, Hirotsugu¹; NINAGAWA, Kiyotaka¹

¹ 岡山理科大学

¹Okayama University of Science

Enstatite in meteorites occasionally shows various cathodoluminescence (CL) emissions with red, reddish purple and blue, whereas terrestrial enstatite has almost no CL emission. We have confirmed several luminescent enstatite in enstatite chondrite (E-chondrite) and enstatite achondrite (Aubrite). In this study, we have conducted to clarify the luminescence centers of CL emissions in extraterrestrial enstatite compared to the CL of terrestrial enstatite.

The polished thin sections of E-chondrites (Sahara 97096, Sahara 97121, Dar al Gani 734 and Y 86004) and Aubrite (Al Haggounia 001) were used for CL measurements. Color CL images were obtained using a cold-cathode type Luminoscope with a cooled-CCD camera. CL spectroscopy was made by a SEM-CL system, which is comprised of SEM (JEOL: JSM-5410LV) combined with a grating monochromator (OXFORD: Mono CL2). The CL emitted from the samples was dispersed by a grating (1200 grooves/mm), and recorded by a photon counting method using a photomultiplier tube. All CL spectra were corrected for total instrumental response, which was determined using a calibrated standard lamp.

Color CL imaging reveals various types of CL emissions with red, reddish purple and blue in the extraterrestrial enstatite. The CL spectra of these enstatite show a broad emission band at 670 nm in a red region, which is assigned to an impurity center derived from activated divalent Mn ion substituted for Mg, and a broad emission band at around 400 nm in a blue region, which might be related to a defect center possibly assigned to "intrinsic defect center" derived during crystal growth.

CL spectra were converted into energy units for spectral deconvolution using a Gaussian curve fitting, because one Gaussian curve in energy units should correspond to one specific type of emission center (Stevens-Kalceff, 2009). The deconvoluted components can be assigned to the emission centers related to impurity centers of trivalent Cr ion at 1.64 eV and divalent Mn ion at 1.86 eV and two defect centers at 2.71 and 3.18 eV. The emission component at 3.18 eV might be attributed to the defect center of structural distortion by the substitution of Al ion for Si in a tetrahedral site, which is possible to be in the process of crystal growth at high temperature in its parent body (e.g., the rocks hosting Al-rich enstatite formed at depths from 25 km to 130?200 km in the lunar rock; Nazarov et al., 2011). Al contents in blue luminescent enstatite are higher than that in red luminescent one. Blue emission center can be detected in the CL of terrestrial samples.

Keywords: Enstatite, Cathodoluminescence, E-chondrite, Emission center

高圧氷の水素自己拡散 Self-diffusion of hydrogen in high-pressure ices: Preliminarily results

野口直樹^{1*}; 奥地拓生¹; 富岡尚敬²
NOGUCHI, Naoki^{1*}; OKUCHI, Takuo¹; TOMIOKA, Naotaka²

¹ 岡山大学地球物質科学研究センター, ² 海洋研究開発機構高知コア研究所
¹Institute for Study of the Earth's Interior, Okayama University, ²Japan Agency for Marine-Earth Science and Technology

High-pressure ices are the primary constituents of mantles of the large icy bodies such as some of Galilean satellites and Edgeworth-Kuiper Belt Objects. Understanding self-diffusion of hydrogen in these high-pressure ices is essential to discuss about mantle dynamics of the large icy bodies because it controls rheology of these ices. In addition, diffusive properties of high-pressure ices are also an interesting topic in the field of high-pressure material science. Shortening of intermolecular distance with increasing pressure induces drastic changes of hydrogen-bonding property such as proton tunneling, proton symmetrization (Benoit et al. 1998), hydrogen sublattice melting (Cavazzoni et al. 1999), and proton hopping transition (Noguchi et al. 2014). Whether these changes of hydrogen bonding affect hydrogen diffusion or not is a major subject in the proton dynamics at high pressure. To elucidate these questions, we have carried out an experiment to determine hydrogen diffusion coefficients of the high-pressure ices using a diamond anvil cell (DAC) and Raman spectroscopy.

The diffusion couples have been prepared from polycrystalline H₂O and D₂O ices prepared within a sample chamber of DAC. The diffusion experiments of these couples were carried out using an electric furnace. Temperatures were set in a range between 400 K and 500 K. After keeping the DAC in the furnace for a few days, Raman mapping measurements of the diffusion couples were carried out at room temperature. Two-dimensional diffusion profiles of deuterium were determined using quantitative curves for deuterium concentration. The quantitative calibration curves were functions as the relative area of Raman band of OH stretching mode to that of OD stretching mode, or Raman shifts of OH and OD stretching modes. Preliminarily results will be reported in our presentation.

キーワード: 高圧氷, 自己拡散, レオロジー, ラマン分光
Keywords: high-pressure ices, self-diffusion, rheology, Raman spectroscopy

Rietveld法による分子篩効果がモルデナイトの細孔構造変化に及ぼす影響 Structure investigation of mordenite induced by molecular sieve using the Rietveld method

菅野 音和^{1*}
SUGANO, Neo^{1*}

¹ 筑波大学生命環境学群地球学類
¹Life & Env. Sci. Univ. of Tsukuba

[はじめに]

天然や合成された物を含めて数多くの種類が存在しているゼオライトは、Si/AIO₄四面体の三次元的なフレームワーク構造から成り立ち、その多くがフレームワーク構造の細孔に水分子を内包した構造を有している。また、Si₄⁺とAl₃⁺の置換に起因する負電荷を補填する為、様々な陽イオンや分子を孔内に吸着、保持する分子篩作用と呼ばれる特性を持つ。このような高い陽イオン吸着能力を活用して、ゼオライトは様々な分野において幅広く注目されている。

ゼオライトグループのひとつであるモルデナイト [(Na₂, Cs, K₂)₄(Al₁₈Si₄₀)O₉₆·28H₂O] (Martucci et al., 2003) は、放射性セシウムと放射性ストロンチウムに対して高い吸着能力を持つことが知られており (Valcke et al., 1997)、放射性廃棄物の除染方法の有力な候補とされている。しかしながら、Csに対して高い吸着特性を有するモルデナイトのCs⁺イオンに対する分子篩作用を結晶構造というミクロな視点から扱った研究は少なく、分子篩作用と結晶構造変化の関係性については未だ不明瞭な点が多い。本研究は、モルデナイトのCs⁺イオン吸着による結晶構造変化を明らかにする為にRietveld解析を行った。

[実験方法]

実験に用いた試料は、Cs⁺イオン濃度を0.010, 0.10, 1.0, 2.0, 4.0, 8.0, 10.0, 30.0g/lに調整したCsCl水溶液100mlと、1.0gの合成モルデナイトをイオン交換させる事によってCs⁺イオンをモルデナイトに吸着させた。イオン交換は速度32rpmの振盪運動によって48時間かけて行われ、水溶液の温度は概ね20°Cに保たれた。その後、Cs⁺イオン吸着前後のモルデナイトの粉末X線回折測定結果を実施した。測定は全自動多目的X線回折装置を使用し、照射X線源にCuK α 線($\lambda = 1.54056\text{\AA}$)、測定範囲は $5^\circ \leq 2\theta \leq 120^\circ$ でスキャン速度とスキャン幅はそれぞれ $4^\circ/\text{min}$ と 0.02° に設定して測定を行った。続いて、Rietveld解析によって結晶構造精密化を行い、陽イオン吸着メカニズムと分子篩作用による結晶構造変化の関係性を明らかにした。Rietveld解析にはRietan FPを使用した。

[結果と考察]

イオン交換実験の結果、モルデナイトをCsCl水溶液に加えなかった時の平衡pH値が 3.44 ± 0.02 であるのに対して、加えた場合の平衡pH値は $2.70-3.09 \pm 0.02$ であった。この平衡pH値の低下は、溶液中のCs⁺イオンがモルデナイトの孔構造中のH⁺イオンとイオン交換した事を示している。Rietveld解析の結果、モルデナイトはCs⁺イオンを吸着すると格子定数が等方的に収縮する性質を示し、単位格子体積が $V = 2880(12)\text{\AA}^3$ から $V = 2836(12)\text{\AA}^3$ へと、最大で $44(17)\text{\AA}^3$ 減少した。モルデナイトの分子篩作用は、Cs⁺イオンを占有するSi/AIO₄四面体フレームワークの12員環(12MRc)と8員環(8MRc)の伸縮によって特徴付けられた。孔構造が最も大きい12MRcでは、Cs⁺イオンを吸着するとCs⁺イオンとフレームワークとの静電引力及び、12MRc内の水分子の脱離によって員環が収縮し、b軸方向の径が $8.90(4)\text{\AA}$ から $8.59(7)\text{\AA}$ へと、最大で $0.31(8)\text{\AA}$ 収縮する特徴が見られた。つまり、12MRcでは員環の収縮による効率的な分子篩作用が働く事によって、Cs⁺イオンが優先的に分配される。一方、12MRcと隣接し孔構造が12MRcよりも小さな8MRcでは、Cs⁺の吸着と孔構造の変化に有意な相関は観察されなかった。つまり、8MRcではCs⁺イオンとの静電引力ではなく12MRcの構造変化に強く支配されて員環が伸縮するため、有効な分子篩作用は働いていない事が示唆された。このため、8MRcのCs⁺イオンの席占有率は12MRcよりも常に低く、伸縮の程度も誤差の範囲内に収まっている事が明らかになった。

キーワード: モルデナイト, 分子篩作用, Rietveld 解析
Keywords: Mordenite, Molecular sieve, Rietveld refinement

ダイヤモンドアンビルセルを用いた上部マントル無水鉱物の高圧その場 IR 観察 In situ high pressure IR spectroscopic observations on the upper mantle anhydrous minerals using diamond anvil cell

櫻井 萌^{1*}; 辻野 典秀²; 館野 繁彦³; 鈴木 敏弘¹; 芳野 極²; 河村 雄行⁴; 高橋 栄一¹
SAKURAI, Moe^{1*}; TSUJINO, Noriyoshi²; TATENNO, Shigehiko³; SUZUKI, Toshihiro¹; YOSHINO, Takashi²;
KAWAMURA, Katsuyuki⁴; TAKAHASHI, Eiichi¹

¹ 東京工業大学大学院理工学研究科地球惑星科学専攻, ² 岡山大学地球物質科学研究センター, ³ 東京工業大学地球生命研究所, ⁴ 岡山大学大学院環境生命科学研究科循環環境学専攻

¹Earth and Planet. Sci., Tokyo Tech, ²ISEI, Okayama Univ., ³ELSI, Tokyo Tech., ⁴Environmental and Life Sci., Okayama Univ.

Most nominally anhydrous minerals (NAMs) in the Earth's upper mantle can contain small amounts of hydrogen (i.e. "water"), structurally bond as hydroxyl. Structurally bounded water causes important influences on many physical properties of mantle rocks. The influence seems to be controlled by hydrogen atoms positions in crystal structure. In most of previous researches, hydrogen atoms positions have been estimated by comparison between the theoretically calculated IR spectra and the experimental results, which obtained at ambient pressure [1, 2]. Therefore, the influence of pressure on hydrogen atom positions has not been identified yet. However, the physical properties relating to hydrogen atom (electric conductivity, viscosity and more), have been measured at high pressure conditions. Thus it is important to clarify the influence of pressure on hydrogen atoms positions.

To observe the influence of pressure on IR spectra, high-pressure experiments have been conducted at pressures of 0.4 – 9.0 GPa at room temperature. The experiments were performed with diamond anvil cell by using natural olivine (Ol) and synthetic forsterite (Fo) as starting materials. The pressure medium was KBr powder or fluorinert. Pressure was determined by ruby fluorescence method [3]. The IR spectra were obtained with a vacuum type Fourier transform infrared spectrometer (Jasco: FT-IR6100, IRT5000).

Clear OH stretching vibration bands could be observed for samples with water concentration over ~100 wt.ppm. The non-polarized IR spectrum of synthesized Fo showed four bands; two stronger ones at 3610, 3575 cm^{-1} and two weaker bands at 3550, 3475 cm^{-1} at ambient pressure. The band at 3475 cm^{-1} disappeared in the spectrum of randomly oriented Fo at ≥ 5.6 GPa. The band at 3610 cm^{-1} shifted to low wavenumber with increasing pressure. After decompression, the spectrum return to the almost same position and intensity before increasing pressure. Thus it indicates that these bands shift is a reversible change.

The polarized to *a*-axis IR spectrum of natural Ol showed three bands; 3610, 3598 and 3575 cm^{-1} at ambient pressure. The band at 3610 cm^{-1} shifted to low wavenumber and became weaker with increasing pressure. The band at 3575 cm^{-1} shifted to high wavenumber, which results is opposite to the band at 3610 cm^{-1} , and also became weaker with increasing pressure. The polarized to *b*-axis IR spectrum of natural Ol showed two bands; 3598 and 3575 cm^{-1} . The band at 3598 cm^{-1} did not change with increasing pressure. In this experiment, the diamond anvils touched sample directly above 8 GPa, so we could not observe the spectrum after decompression.

[1] Umemoto et al.: *Am. Min.*, 96, 1475-1479, 219 (2011) [2] Sakurai et al.: *J. Comput. Chem. Jpn.* [3] Mao et al.: *J. Appl. Phys.* 49, 3276-3283 (1978)

キーワード: FT-IR, 圧力効果, 無水鉱物, 上部マントル, 高圧その場観察

Keywords: FT-IR, Pressure effect, Nominally anhydrous minerals, Upper mantle, In situ experiment

放射光 X 線回折法による $\text{Al}_{65}\text{Cu}_{20}\text{Fe}_{15}$ 正 20 面体準周期結晶の安定性に関する研究 Study on the stability of the $\text{Al}_{65}\text{Cu}_{20}\text{Fe}_{15}$ icosahedral quasicrystal using Synchrotron X-ray diffraction method

高木 壮大^{1*}; 興野 純²

TAKAGI, Sota^{1*}; KYONO, Atsushi²

¹ 筑波大学生命環境学群地球学類, ² 筑波大学大学院生命環境科学研究科地球進化科学専攻

¹College of Geoscience, School of Life and Environmental Sciences, University of Tsukuba, ²Graduate School of Life and Environmental Sciences, University of Tsukuba

The stability of the $\text{Al}_{65}\text{Cu}_{20}\text{Fe}_{15}$ icosahedral quasicrystal at high pressure and high temperature has been investigated using synchrotron X-ray diffraction method. High pressure *in situ* XRD experiments were performed up to 104 GPa, and high pressure and high temperature *in situ* XRD experiments were performed at the pressure points of 11, 24, 33, 57, 67, 104 GPa up to temperature of about 2500 K. The high pressure experiments revealed that five characteristic XRD peaks of the $\text{Al}_{65}\text{Cu}_{20}\text{Fe}_{15}$ icosahedral quasicrystal remained up to 104 GPa at room temperature, while a new peak appeared at the point of $d = 2.90 \text{ \AA}$ above 89 GPa. The six-dimensional lattice parameter, a_{6D} , was continuously contracted from 12.5 \AA to 11.2 \AA with pressure. The bulk modulus of the $\text{Al}_{65}\text{Cu}_{20}\text{Fe}_{15}$ icosahedral quasicrystal started to change around 70 GPa. This result suggested that the $\text{Al}_{65}\text{Cu}_{20}\text{Fe}_{15}$ icosahedral quasicrystal was transformed to high pressure phase at about 70 GPa. The high pressure and high temperature experiments showed that a different phase (high-temperature phase) occurs as a function of the temperature. The phase boundary between the $\text{Al}_{65}\text{Cu}_{20}\text{Fe}_{15}$ icosahedral quasicrystal and its high temperature phase was risen with pressure, such as 865 K at 11 GPa, 1402 K at 24 GPa, 1758 K at 33 GPa, 1963 K at 57 GPa, 2050 K at 67 GPa, 2080 K at 104 GPa. In a series of the study, the $\text{Al}_{65}\text{Cu}_{20}\text{Fe}_{15}$ icosahedral quasicrystal was melted completely only when it was heated to 2385 K at 11 GPa. From the present study, it was suggested that mineral icosahedrite ($\text{Al}_{63}\text{Cu}_{24}\text{Fe}_{13}$), the first natural-occurring quasicrystal, was formed at pressure range from 5 GPa to 70 GPa, and at temperature range from 1500 K to 2200 K. This study can be a clue to solve the question of where and how the icosahedrite was formed.

キーワード: $\text{Al}_{65}\text{Cu}_{20}\text{Fe}_{15}$ 正 20 面体準周期結晶, icosahedrite, 安定性, 高温高圧, XRD

Keywords: $\text{Al}_{65}\text{Cu}_{20}\text{Fe}_{15}$ icosahedral quasicrystal, icosahedrite, stability, high pressure and high temperature, XRD

粒子画像解析による火山灰の加熱形状変化の観察 Observation of morphological behavior with heating of volcanic ash by in situ particle image analysis

浜田 寛之^{1*}; 金附 紳一郎²; 早内 愛子¹; 笹倉 大督¹

HAMADA, Hiroyuki^{1*}; KANATSUKI, Shinichiro²; HAYAUCHI, Aiko¹; SASAKURA, Daisuke¹

¹ スペクトリス株式会社 マルバーン事業部, ² ジャパンハイテック株式会社

¹Malvern Instruments, A division of Spectris Co., Ltd., ²Japan High Tech Co., Ltd.

1. Introduction

An *in-situ* observation to particle morphology under any perturbations is well used to understand physical chemistry behavior of mineral particles. With using by a heating response as a one of perturbation is interesting to investigate to melting and crystallinity of minerals. One of drawback to particle morphology investigation by a manually microscope is a qualitative approach rather than quantitative approach.

Our group has reported particle characterization and classification of a volcanic ash fine particle using by images for the purpose of determining particle size distribution which is based on described in ISO13322. The particles are appropriately dispersed and fixed on an optical microscope implemented an automated real time particle image analysis function on software. This report will be discussed for observation of morphological behavior with heating of volcanic ash by in situ particle image analysis.

2. Material and Method

In this study, the volcanic ash was sampling from Ito flow in Kagoshima. As a statistical particle image analysis, an automated particle image analyzer, Morphologi G3-SE (Malvern Instruments) was used for evaluation of particle size and shape. The observation mode was reflectance mode magnification was 75x in total magnification. The sample was dispersed with SDU (Sample Dispersion Unit) which attached Morphologi G3-SE. Number of measured particles was several hundred and a parameter filter function on software was used based on shape and pixel number of particle image. As a heat stage, Linkam stage TS1500 (Japan Hightech Co., Ltd.) was use for sample heating up to 1500 °C. A sample particle was dispersed on a platinum sample cell by SDU.

3. Result and Discussion

As a result of feasibility study, Fig.1 shows the observed images at 30 °C, 500 °C, 1000 °C, and 1500 °C. No change was observed between 30 °C and 1000 °C. However, the significant change of particle morphology by melting was observed between 1000 °C and 1500 °C. Refer to result of feasibility test, the temperature range from 1000 °C to 1500 °C is appropriate for this investigation.

4. Conclusion

In summarize of this study, it was possible to observe particle morphology change by heating. This report will be more discussed about the application and the capability for more quantitative investigation by particle image analysis.

キーワード: 火山灰, 顕微鏡法, 粒子画像解析, 粒子径, 粒子径分布

Keywords: volcanic ash, microscopy, particle image analysis, particle diameter, particle distribution

SMP42-P14

会場:コンベンションホール

時間:5月26日 18:15-19:30

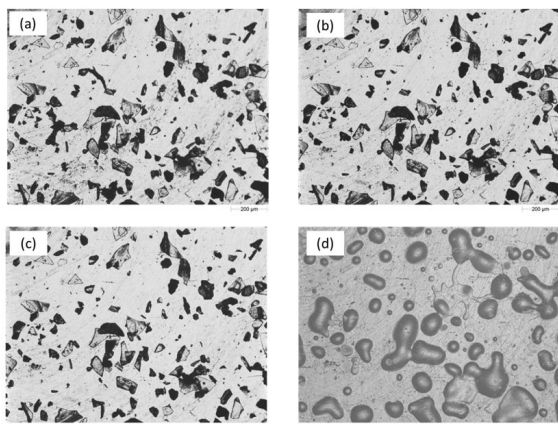


Fig.1 Particle morphology change under heating. (a)30°C (b)500°C (c)1000°C (d)1500°C

低温高圧下における H₂O の磁化率測定 Magnetic measurement of H₂O at low-temperature and high-pressure

近藤 忠^{1*}; 懸田 隆史¹; 谷口 年史¹
KONDO, Tadashi^{1*}; KAKEDA, Takafumi¹; TANIGUCHI, Toshifumi¹

¹ 大阪大学大学院理学研究科

¹ Graduate School of Science, Osaka University

Water ice is universal material in space and has fifteen polymorphs reported so far. Because of difficulty in detection of subtle structure change corresponding to hydrogen shift, and slow kinetics of low-temperature ice, some phase boundaries at low temperature are still not confirmed experimentally, which is very important information in planetary science. In this study, we tested a possibility of new method for studying structural change of ice using magnetic measurement at low-temperature and high-pressure. H₂O is diamagnetic substance, and the signal intensity of magnetic susceptibility is not detectable if we use a conventional method of magnetic measurement. However, positional ordering of hydrogen atoms should change the spin state of ice. Therefore, we can expect finite change in magnetic susceptibility.

Magnetic measurements were conducted in Superconducting Quantum Interference Device magnetometer (SQUID, MPMS-7, Quantum design). We measured the magnetic moment of ice at temperature below room condition. The measurement was also conducted at high-pressure condition to 0.2GPa to detect phase boundary between phase IX and phase I. Highly purified water with 5 M ohm resistivity or salted waters was used as starting sample in the Teflon capsule with /without a piston cylinder type high pressure cell made of beryllium copper alloy. After many trials of accurate evaluation of magnetic moment of all material surrounding sample as background signal to be subtracted, we measure the signal with water ice in the capsule. The magnetic field applied was 1T. The sample was first cooled to around 100K, then, the temperature elevated to room condition at the rate of 0.25K/s.

Solid-liquid transition of pure water was reproducibly detected with abrupt decrease of magnetic susceptibility. In the case of salt water, magnetic susceptibility decreased gradually with a temperature width as figured by thermodynamics. In the high-pressure run, we found an another jump in the profile of magnetic susceptibility measurement. The condition was close to solid-solid phase boundary proposed. We will report further detail of the experiments as possible detection of phase change in low-temperature water ice.

Keywords: water ice, magnetic measurement, high pressure, phase transition, SQUID